Available online at www.sciencedirect.com

ScienceDirect

Procedia Manufacturing 26 (2018) 164–172

Procedia MANUFACTURING

www.elsevier.com/locate/procedia

46th SME North American Manufacturing Research Conference, NAMRC 46, Texas, USA

The role of tool presetting in milling stability uncertainty

Milton Vieira Junior[a], Elesandro Antonio Baptista[a], Luciana Araki[a], Scott Smith[b], Tony Schmitz[b]*

[a]*Universidade Nove de Julho, Programa de Pós-graduação em Engenharia de Produção, São Paulo, Brazil*
[b]*UNC Charlotte, Mechanical Engineering and Engineering Science, Charlotte, NC 28223, USA*

* Corresponding author. Tel.: +1-704-687-5086.
E-mail address: tony.schmitz@uncc.edu

Abstract

This paper describes the relationship between presetter tool extension length and diameter measurements, the tool point frequency response function (FRF), and milling stability. Three scenarios are considered: 1) the tool extension from the holder face is controlled during setup and measured by the presetter for validation; 2) the tool extension length from the holder face is not controlled during setup and measured to update the tool information in the part program; and 3) the measured extension length is used to update the stability boundary prediction and corresponding operating parameters in the part program. Example presetting results are provided to establish the associated measurement uncertainty. Next, the receptance coupling substructure analysis (RCSA) technique is used within a Monte Carlo simulation to establish the tool point FRF uncertainty as a function of the tool extension length and diameter uncertainty. Finally, the distribution in the tool point FRF is propagated to uncertainty in the milling stability limit. Each of the three scenarios is evaluated to understand their implications for milling stability.

Peer-review under responsibility of the scientific committee of the 4th International Conference on System-Integrated Intelligence.

Keywords: Milling; stability; chatter; tool presetting; receptance coupling substructure analysis; frequency response function

1. Introduction

Tool management represents a key consideration in modern subtractive manufacturing organizations. Its importance continues to grow with: the increasing number of tools available from multiple vendors; new cutting edge materials and coatings; and the large number of tools kept in storage within automated tool magazines located on the computer numerically controlled (CNC) machining centers [1]. Successful tool management requires that the proper tool is selected in each instance in order to make full use of the CNC machine's capabilities. Activities required to meet this objective include inventory control, either in

2351-9789
Peer-review under responsibility of the scientific committee of the 4th International Conference on System-Integrated Intelligence.
10.1016/j.promfg.2018.07.023

a centralized fashion or localized to a flexible manufacturing cell, and accurate tool setup. Inventory can be effectively monitored using bar code labels or electronically programmable tags (such as RFID [2]). Tool setup includes proper geometric assembly of the tooling components (e.g., a collet holder and solid carbide end mill) and may be completed remotely from the CNC machine or directly on the machine [3]. On-machine testing can include tool length and diameter validation, wear evaluation, and broken tool checks.

Proper tool setup is critical for two primary reasons: 1) the tool diameter and offsets must be properly represented in the computer-aided manufacturing (CAM) part program to provide the appropriate geometric tool motions relative to the part; and 2) the material removal process performance depends on the tool geometry, including the assembly's dynamic flexibility and runout of the cutter teeth (for rotating tools). The structural dynamics affect the process stability (i.e., the potential presence of chatter, or self-excited vibrations) and part accuracy (through forced vibrations during stable cutting) [4]. Runout directly influences the machined surface finish [5-6].

Current tool measurement practices primarily focus on geometrical concerns. That is, the part program is written with a specific tool length in mind, but the physical tool may be different if the setup process is not well controlled. When the tool is preset, or when the tool is loaded into the machine, its true length is measured (for example, by touch-off in the spindle). A correction for the difference between planned and true tool length (tool length compensation) is entered into the controller and the part program is adjusted in real time to account for the geometrical difference. However, this common practice ignores the fact that different tool lengths lead to different cutting performance. In the current environment where the tool setting is not under tight control, the tool use may differ from the one that was planned in many ways: length, number of flutes, helix angle, tool material/coating, and so on. The user is supported only in correcting for the geometrical difference. This paper describes a method to recognize and accommodate the performance difference associated with the geometry difference.

Besides technological influences, presetting can also have managerial influences over both productive and unproductive times, not only during setup. Therefore, an effective presetting operation can achieve greater productivity as a result of increasing availability of machines [7].

The tool point frequency response function, or FRF, describes the structural dynamics of a selected tool-holder-machine combination [8]. It must be known to enable the pre-process selection of machining parameters that avoid chatter and provide acceptable geometric accuracy. In milling, for example, the tool's extension from the holder strongly influences the tool point FRF. Because this extension must be set for ER/TG collets, thermal shrink fit, hydraulic, and other tool-holder interfaces, tool presetting is an integral component of high productivity machining.

The purpose of this study is to identify the relationship between tool presetting and process stability for peripheral end milling operations. The paper is organized as follows. First, three options for the use of tool presetting data are defined. Second, example presetting results are provided to establish the associated measurement uncertainty. Third, the receptance coupling substructure analysis (RCSA) technique is used to predict the tool point FRF as a function of the tool length and diameter. Fourth, variation in the tool point FRF is propagated to uncertainty in the milling stability limit (to avoid chatter). Finally, conclusions are presented.

2. Use of tool presetting data

There are three options for the use of tool presetting data, including the tool extension and diameter. These are:

1. The tool extension from the holder face is controlled during setup. In this scenario, the extension after a tool change is nominally the same and the presetter is only used to verify the length and diameter and make minor adjustments to the tool parameters in the part program.
2. The tool extension length from the holder face is not controlled during setup. In this case, the tool length after a tool change can be significantly different than the previous tool setup. The presetter is then used to measure the actual length, verify the diameter, and change the tool parameters in the part program.
3. The presetter is used to measure the extension length and verify the diameter. The measured extension length is used to update the stability boundary prediction and, subsequently, modify the spindle speed to obtain stable behavior for a selected axial depth of cut.

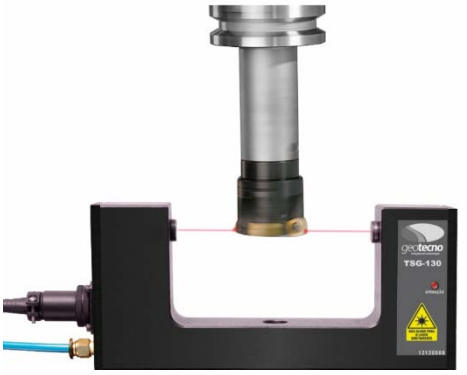

Fig. 1. Photograph of TSF-130 tool presetter [8].

3. Tool presetting measurements

To establish the uncertainty in tool presetting measurements, a study was competed using a Geotecno TSG-130 laser-based tool presetting station [9]; see Fig. 1. The tool assembly was composed of a Sandvik Coromill 390 square shoulder, two insert milling cutter (Sandvik R390-020A20-11L) clamped in a Sanches Blanes BT-40 ER collet holder (34.55.040).

The following steps were completed to collect the tool presetting measurement data.

- The machine was turned on and a program was executed for 30 minutes to enable the machine to reach thermal equilibrium.
- After this pre-heating step, a referencing cycle was performed to report the position of the laser beam to the CNC controller. In this cycle, a reference pin with known dimensions was used.
- Once the laser beam was referenced, experiments were completed to measure the tool extension length and diameter using three different: 1) spindle speeds, {1400, 1800, and 2200} rpm; and 2) approach velocities, {2, 4, and 6} mm/min (selected using [10]). Ten trials were completed for all nine combinations of spindle speed and velocity (feed rate). This yielded a total of 90 tests. The measured parameters are shown in Fig. 2. These included a reference location at the spindle (R), the holder length (h_2), the holder and tool length (h_1), and the tool diameter (d).
- Parameters h_1, h_2, and d were measured with the spindle rotating, while R was measured with the spindle stationary.

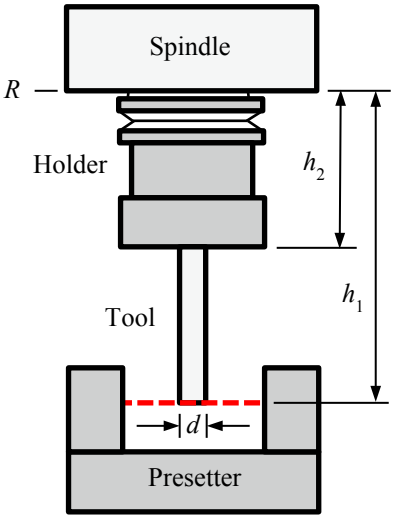

Fig. 2. Geometric parameters measures by the tool presetter.

Measurement results are displayed in Figs. 3-6. The mean values are reported. One standard deviation error bars are also included, where the standard deviations were calculated using the 10 measurement trials for each spindle speed-velocity pair. To determine the tool extension length, the difference between h_1 and h_2 was calculated. This result is presented in Fig. 7.

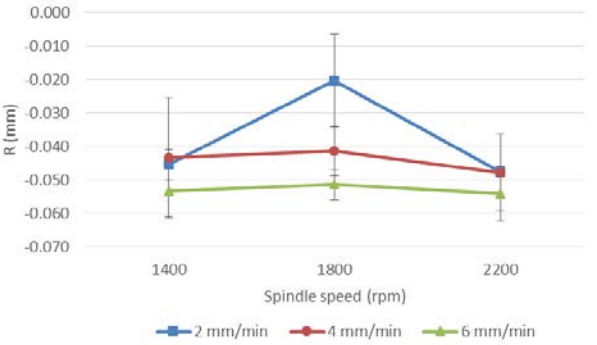

Fig. 3. Tool presetter measurements for R.

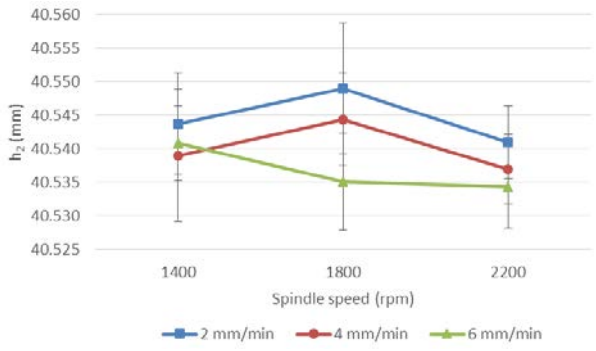

Fig. 4. Tool presetter measurements for h_2.

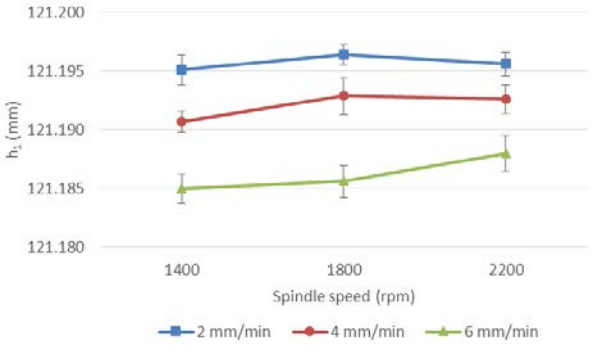

Fig. 5. Tool presetter measurements for h_1.

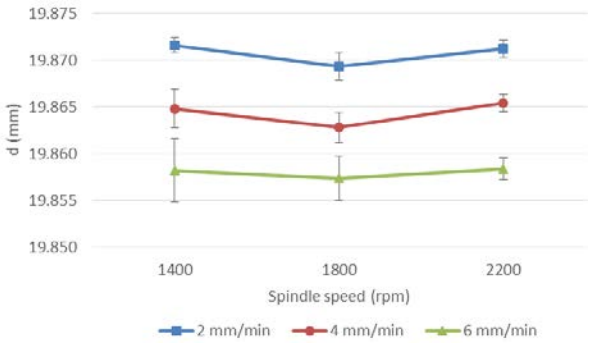

Fig. 6. Tool presetter measurements for d.

Figures 3-6 show modest trends in the measured parameters with approach velocity. No consistent trends are apparent with changes in spindle speed. Figure 7, on the other hand, shows no clear trend with either velocity or spindle speed. The mean value of d for all 90 tests was 19.8644 mm with a standard deviation of 0.0056 mm. The mean value of $h_1 - h_2$ for all 90 tests was 80.6508 mm with a standard deviation of 0.0080 mm.

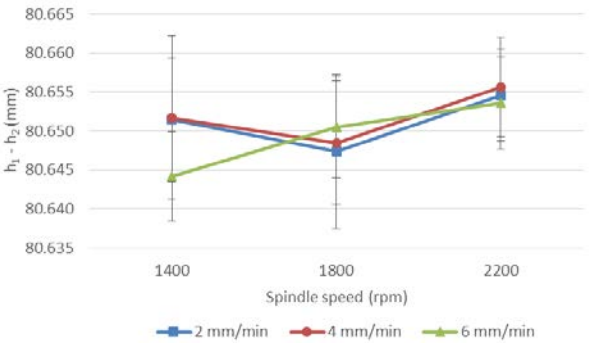

Fig. 7. Tool presetter measurements for $h_1 - h_2$.

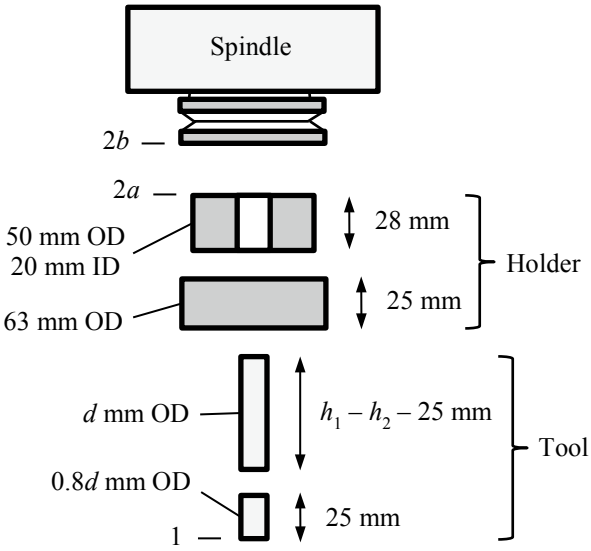

Fig. 8. Tool-holder geometry for RCSA.

4. RCSA

Given the tool setup measurement values, the tool point FRF can be determined using RCSA. RCSA is a frequency domain, analytical procedure used to couple component FRFs (or receptances) in order to predict the assembly receptances [11-12]. In this work, the free-free boundary condition receptances for the tool and holder are rigidly coupled to the spindle receptances; see Fig. 8, where the measured tool dimensions are included as d and $h_1 - h_2$ and the inserted portion of the tool at the free end was described using an effective diameter that was 80% of

the solid shank diameter. The material properties for both the tool and holder were: 200 GPa elastic modulus, 7800 kg/m^3 density, and 0.29 Poisson's ratio.

Using rigid compatibility and equilibrium conditions, the assembly direct receptance, $H_{11} = \frac{Y_1}{F_1}$, at assembly coordinate Y_1 is written as a function of the component receptances at coordinates 1, $2a$, and $2b$; see [4] for the derivation. The required direct and cross receptances for the free-free tool-holder (coordinates 1 and $2a$) and spindle (coordinate $2b$) components are:

- $h_{11} = \frac{y_1}{f_1}$, $h_{12a} = \frac{y_1}{f_{2a}}$, $h_{2a1} = \frac{y_{2a}}{f_1}$, $h_{2a2a} = \frac{y_{2a}}{f_{2a}}$, and $h_{2b2b} = \frac{y_{2b}}{f_{2b}}$, where y_i is the component displacement and f_j is the (internal) component force
- $l_{11} = \frac{y_1}{m_1}$, $l_{12a} = \frac{y_1}{m_{2a}}$, $l_{2a1} = \frac{y_{2a}}{m_1}$, $l_{2a2a} = \frac{y_{2a}}{m_{2a}}$, and $l_{2b2b} = \frac{y_{2b}}{m_{2b}}$, where m_j is the (internal) component moment
- $n_{11} = \frac{\theta_1}{f_1}$, $n_{12a} = \frac{\theta_1}{f_{2a}}$, $n_{2a1} = \frac{\theta_{2a}}{f_1}$, $n_{2a2a} = \frac{\theta_{2a}}{f_{2a}}$, and $n_{2b2b} = \frac{\theta_{2b}}{f_{2b}}$, where θ_i is the component rotation
- $p_{11} = \frac{\theta_1}{m_1}$, $p_{12a} = \frac{\theta_1}{m_{2a}}$, $p_{2a1} = \frac{\theta_{2a}}{m_1}$, $h_{2a2a} = \frac{\theta_{2a}}{m_{2a}}$, and $p_{2b2b} = \frac{\theta_{2b}}{m_{2b}}$.

The assembly receptances for the tool tip are provided in Eq. 1 [4], where H_{11} is the displacement-to-force receptance required for the machining stability analysis.

$$\begin{bmatrix} H_{11} & L_{11} \\ N_{11} & P_{11} \end{bmatrix} = \begin{bmatrix} h_{11} & l_{11} \\ n_{11} & p_{11} \end{bmatrix} - \begin{bmatrix} h_{12a} & l_{12a} \\ n_{12a} & p_{12a} \end{bmatrix} \left(\begin{bmatrix} h_{2a2a} & l_{2a2a} \\ n_{2a2a} & p_{2a2a} \end{bmatrix} + \begin{bmatrix} h_{2b2b} & l_{2b2b} \\ n_{2b2b} & p_{2b2b} \end{bmatrix} \right)^{-1} \begin{bmatrix} h_{2a1} & l_{2a1} \\ n_{2a1} & p_{2a1} \end{bmatrix} \quad (1)$$

The tool-holder component receptances can be obtained from measurements or models. Two modeling options are the Euler-Bernoulli and Timoshenko beams. Here, the one-dimensional Timoshenko beam model was implemented to find the free-free boundary condition receptances. This requires a numerical solution of the partial differential equation displayed in Eq. 2 [13], where ρ is the density, A is the beam's cross-sectional area, G is the shear modulus, and $\hat{k}$ is a shape factor that depends on the beam's cross section [14].

$$\left(\frac{\partial^2 y}{\partial t^2} + \frac{EI}{\rho A}\frac{\partial^4 y}{\partial x^4}\right) + \left(\frac{\rho I}{\hat{k}AG}\frac{\partial^4 y}{\partial t^4} + \frac{EI}{\hat{k}AG}\frac{\partial^4 y}{\partial x^2 \partial t^2}\right) - \left(\frac{I}{A}\frac{\partial^4 y}{\partial x^2 \partial t^2}\right) = 0 \quad (2)$$

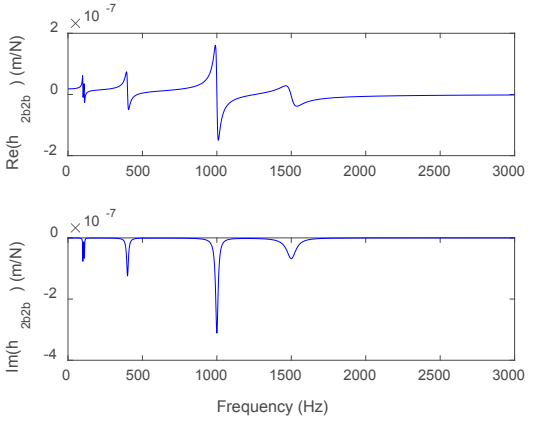

Fig. 9. Spindle displacement-to-force receptance h_{2b2b}.

The spindle displacement-to-force receptance, h_{2b2b}, is shown in Fig. 9. Five modes are observed at {100, 110, 400, 1000, and 1500} Hz. The remaining rotational spindle receptances were defined using the technique described in [15].

To determine the variation in the tool point FRF due to the uncertainties in the tool diameter and extension length presetter measurements, a Monte Carlo simulation was developed. In each iteration of the simulation, the tool diameter and extension length were sampled from normal distributions. These normal distributions were defined using the mean values from the complete measurement set (90 total measurements). The standard deviations for the normal distributions was taken to be the standard deviations from the measurements multiplied by a coverage factor of 2.

Given the sampled tool diameter and extension length, the tool model was defined (see Fig. 8). The spindle receptances were then rigidly coupled to the holder and tool free-free receptances to predict the assembly response. This process was completed many times to determine the corresponding distribution in the tool point FRF.

The result from 1000 Monte Carlo simulation iterations is shown in Fig. 10. A higher magnification view of the real and imaginary parts near the dominant natural frequency is displayed in Fig. 11. It is seen that the tool presetter measurement uncertainty is sufficiently small that there is only minor variation in the tool point FRF.

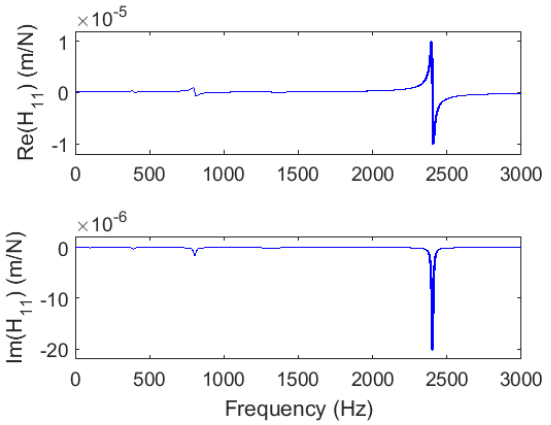

Fig. 10. Distribution in tool point FRF due to uncertainty in tool diameter and extension from presetter measurements.

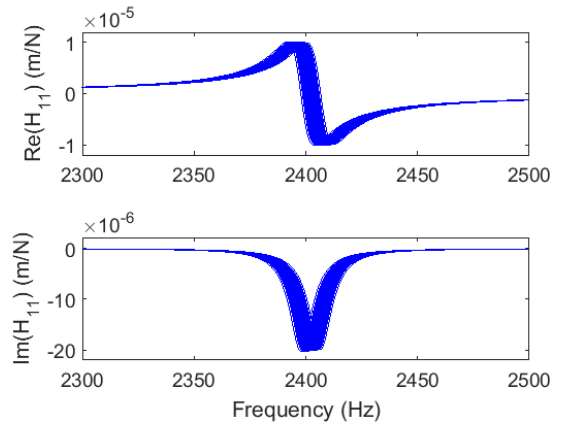

Fig. 11. Distribution in dominant mode for tool point FRF due to uncertainty in tool diameter and extension from presetter measurements.

5. Milling stability limit uncertainty

The Monte Carlo simulation was next extended to determine the variation in the milling stability boundary based on the variation in the tool point FRF. In each iteration, a new stability boundary was defined using the calculated tool point FRF.

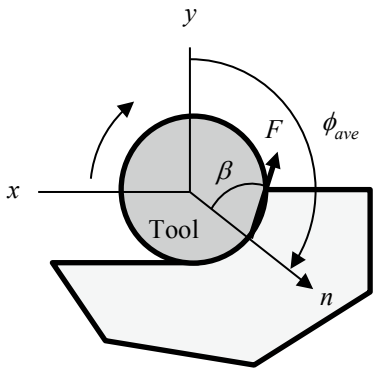

Fig. 12. Geometry for average tooth angle analytical stability analysis.

The average tooth angle analytical stability analysis [4] was applied for 50% radial immersion down milling of 6061-T6 aluminum using the two-insert end mill. The cutting force, F, model used a specific force coefficient, K_s, which relates the resultant cutting force to the chip area, of 750 N/mm^2 and a force angle, β, of 68 deg. Figure 12 displays the cut geometry, where the tool feed is in the negative x direction, ϕ_{ave} is the average tooth angle between the entry and exit angles for the down milling cut, and n is the surface normal direction at the average tooth angle.

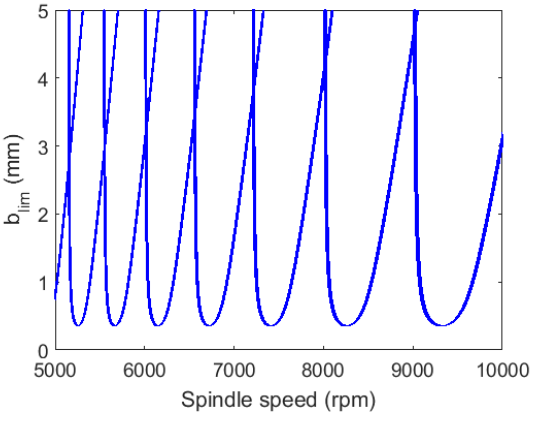

Fig. 13. Stability boundary for tool point FRF variation based on the presetter measurement uncertainty for the tool diameter and extension.

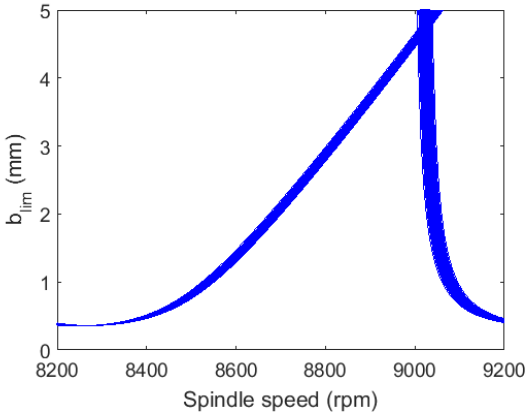

Fig. 14. Magnified view of stability boundary near 9000 rpm for tool point FRF variation based on the presetter measurement uncertainty for the tool diameter and extension.

The Monte Carlo simulation result for the first scenario in Section 2 is presented in Fig. 13. In this case, the extension after a tool change is nominally the same and the presetter is only used to verify the length and diameter and make minor adjustments to the tool parameters in the part program. In Fig. 13, 1000 iterations of the Monte Carlo simulation are displayed, where the limiting axial depth of cut to avoid chatter, b_{lim}, is plotted versus the spindle speed. A higher magnification view of the stability limit near 9000 rpm is shown in Fig. 14. It is observed that the variation is small when the tool extension is controlled and the uncertainty is limited to the presetter measurement uncertainty. For the selected radial depth of cut (50% radial immersion), an axial depth of cut of 3 mm at a spindle speed of 9000 rpm would enable high metal removal rate without chatter.

The previous analysis assumed that the tool geometry varied only by the uncertainty in the presetter measurements. If the tool extension length varies over a much wider range because the length is not well controlled during the tool setup (the second scenario from Section 2), the corresponding variation in the stability boundary is larger.

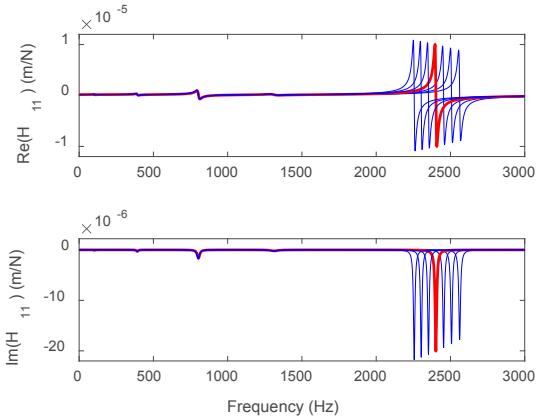

Fig. 15. Tool point FRFs for a ±3 mm variation in the tool extension length. The thicker line represents the FRF for the mean length from the tool presetter measurements.

To explore the sensitivity of the stability boundary to the extension length, the length was varied to define a new tool point FRF and the corresponding stability boundary was calculated. The mean length value from the presetter measurements was varied by ±3 mm in 1 mm increments (seven total lengths). As noted, this exercise matches the second scenario where the tool extension length is not controlled and the presetter is used to update the actual length in the CNC part program (even though the new length may be significantly different than the original length). The mean diameter was used without variation for these calculations. The seven tool point FRFs are displayed in Fig. 15. The response for the mean length from the presetter measurements is identified by the thicker line.

The variation in the stability boundary for the seven FRFs from Fig. 15 is displayed in Fig. 16. It is observed that the stable gap near 9000 rpm is only accessible for the mean extension length. If the machining parameters were selected to be an axial depth of 3 mm at a spindle speed of 9000 rpm (marked by the solid circle in Fig. 16) based on the tool point FRF obtained for the mean extension length, chatter would be obtained for all other extension lengths even though the proper tool parameters would be inserted in the part program based on the presetter measurements. The stability boundary for the mean extension length is identified by the thicker line in Fig. 16.

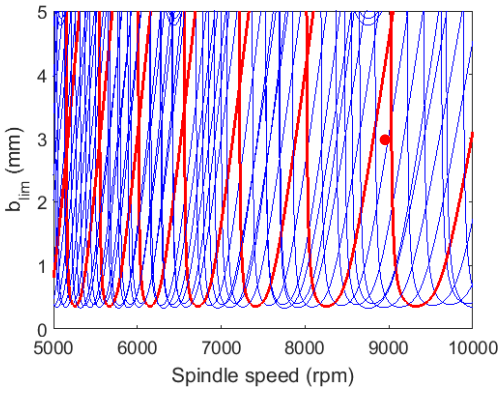

Fig. 16. Stability boundary for tool point FRF variation based on a ±3 mm variation in the tool extension length. The thicker line represents the boundary for the mean length from the tool presetter measurements. The 3 mm axial depth, 9000 rpm operating condition is marked with a solid circle.

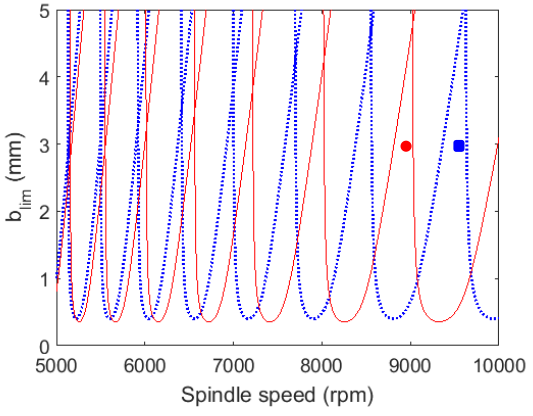

Fig. 17. Stability boundary for the mean tool extension length (solid) and the mean minus 3 mm length (dotted). The 3 mm axial depth, 9000 rpm operating condition (solid circle) is valid for the mean length, while the 9600 rpm spindle speed is required for the mean minus 3 mm length (solid square).

To satisfy the third scenario from Section 2, the extension length measured by the tool presetter must be used to update the stability boundary prediction and, subsequently, modify the spindle speed to obtain stable behavior for the selected axial and radial depths of cut. Consider the case from Fig. 15 when the extension length is the mean minus 3 mm. The shorter length gives the highest natural frequency (i.e., the rightmost FRF from Fig. 15). To represent the third scenario, two stability limits are shown in Fig. 17:

1. the stability limit for the mean extension length (solid line) with a best spindle speed of 9000 rpm at a 3 mm axial depth (marked by a solid circle)
2. the new stability limit for the shorter extension length (dotted line) with an adjusted spindle speed of 9600 rpm to obtain stable cutting conditions at the same 3 mm axial depth (marked by a solid square).

5. Conclusions

This paper explored the relationship between presetter tool extension length and diameter measurements, the tool point frequency response function (FRF), and the corresponding milling stability. Three scenarios were examined: 1) the tool extension from the holder face is controlled during setup and measured by the presetter for validation; 2) the tool extension length from the holder face is not controlled during setup and measured to update the part program; and 3) the measured extension length is used to update the stability boundary prediction and corresponding operating parameters in the part program.

Presetter measurement results were presented and the uncertainty was established using a statistical analysis. For the tool diameter, the standard deviation from 90 separate tests was 0.0056 mm. For the tool extension, the standard deviation was 0.0080 mm.The receptance coupling substructure analysis (RCSA) technique was used to predict the tool point FRF as a function of the spindle dynamics, the holder response, and the tool response based on its extension length and diameter measured by the presetter. The uncertainty in the presetter measurements was propagated to tool point FRF uncertainty using a Monte Carlo simulation. The distribution in the tool point FRF was then used to determine the uncertainty in the milling stability limit. Each of the three scenarios was evaluated to understand their implications for milling stability. It was demonstrated that the RCSA FRF prediction capability enables appropriate milling parameters to be selected for chatter-free operation based on the measured tool extension length.

Acknowledgements

The authors gratefully acknowledge financial support from FAPESP grant number 15/16593-6, NSF CMMI-1561221, and the UNC Charlotte/FAPESP SPRINT program.

References

[1] Eversheim, W., Kals, H.J.J., König, W., van Luttervelt, C.-A., Milberg, J., Storr, A., Tönshoff, H.K., Weck, M., Weule, H. and Zdeblick, W.J., 1991, Tool management: The present and the future, Annals of the CIRP, 40/2: 631-639.

[2] Wang, G., Nakajima, H., Yan, Y., Zhang, X., and Wang, X., 2009, A methodology of tool lifecycle management and control based on RFID, Proceedings of the 2009 IEEE IEEM, 1920-1924.

[3] Beard, T., 1998, Setting tools makes small shop sense, Modern Machine Shop, https://www.mmsonline.com/articles/setting-tools-makes-small-shop-sense.

[4] Schmitz, T. and Smith, K.S., 2009, Machining Dynamics: Frequency Response to Improved Productivity, Springer, New York, NY.

[5] Arizmendi, M., Fernández, J., Gil, A., and Veiga, F., 2009, Effect of tool setting error on the topography of surfaces machined by peripheral milling, International Journal of Machine Tools & Manufacture, 49: 36-52.

[6] Schmitz, T., Couey, J., Marsh, E., Mauntler, N., Hughes, D., 2007, Runout effects in milling: Surface finish, surface location error, and stability, International Journal of Machine Tools & Manufacture, 47: 841-851.

[7] Correr, I., Vieira Junior, M., Silva, J.M.A., Silva, D.S., Costa, A.L., 2011, Statement of losses caused by the presetting of tools by the manual method, In: POMS 22nd Annual Conference Annals, Reno, NV, 1-15.

[8] Schmitz, T. and Smith, K.S., 2012, Mechanical Vibrations: Modeling and Measurement, Springer, New York, NY.

[9] http://geotecno.com.br/produto-2/.

[10] Vieira Junior, M., Pereira, F., Lucato, W., Costa, F.S., 2015, Influence of feed rate and spindle speed on referencing laser tool-setters, Journal of the Brazilian Society of Mechanical Sciences and Engineering, 37: 1015-1028.

[11] Bishop, R.E.D., and Johnson, D.C., 1960, The Mechanics of Vibration, Cambridge University Press, Cambridge, UK.

[12] Schmitz, T. and Duncan, G.S., 2005, Three-component receptance coupling substructure analysis for tool point dynamics prediction, Journal of Manufacturing Science and Engineering, 127/4: 781-790.

[13] Weaver, Jr., W., Timoshenko, P., and Young, D., 1990, Vibration Problems in Engineering, 5th Ed., John Wiley and Sons, New York, NY.

[14] Hutchinson, J., 2001, Shear coefficients for Timoshenko beam theory, Journal of Applied Mechanics, 68: 87-92.

[15] Kumar, U.V. and Schmitz, T., 2012, Spindle dynamics identification for Receptance Coupling Substructure Analysis, Precision Engineering, 36/3: 435-443.